University of Baghdad
College of Engineering
JE
JOURNAL OF ENGINEERING

# Journal of Engineering

journal homepage: www.jcoeng.edu.iq

Volume 30 Number 4 April 2024

# A Comparative Study of the Structural Behavior of Concrete Beams Reinforced with Different Configurations of GFRP and Steel Bars

**Shaysh Aziz Mohammed[1,*], AbdulMuttailb Issa Said[2]**

Department of Civil Engineering, College of Engineering, University of Baghdad, Baghdad, Iraq
Shaysh96@outlook.com[1], dr.abdulmuttalib.i.said@coeng.uobaghdad.edu.iq[2]

## ABSTRACT

This study examined experimentally and numerically the performance of five concrete beams reinforced with longitudinal and transverse bars made of Glass Fiber Reinforced Polymer (GFRP) or steel. All beams had the same dimensions of 2700 mm in length, 180 mm in width, and 260 mm in depth. The beams were classified into two groups with different variables and compared with a reference beam reinforced with longitudinal and transverse steel bars. The first group consisted of two beams with longitudinal GFRP bars and no stirrups, varying the main reinforcement ratio. The second group comprised two beams with longitudinal GFRP bars and transverse GFRP or steel stirrups, varying the stirrup type. The results indicated that the beams with GFRP bars improved their flexural strength for different ratios but had limited shear resistance when using GFRP stirrups because increased deflection causes the number and width of cracks to grow, reducing the shear strength. All the tested beams exhibited linear elastic behavior until failure, with GFRP being more brittle than steel due to no yield point or plastic behavior in GFRP. The numerical simulation of the five beams using ABAQUS software showed good agreement with the experimental data obtained in the laboratory.

**Keywords:** GFRP, Flexural, Deflection, Concrete, Shear.

*Corresponding author
Peer review under the responsibility of University of Baghdad.
https://doi.org/10.31026/j.eng.2024.04.12

Article received: 25/05/2023
Article accepted: 17/08/2023
Article published: 01/04/2024

# دراسة مقارنة للسلوك الإنشائي للعتبات الخرسانية المسلحة بتكوينات مختلفة من قضبان الياف الزجاج البوليميرية والفولاذ

**شايش عزيز محمد*، عبدالمطلب عيسى سعيد**

قسم الهندسة المدنية، كلية الهندسة، جامعه بغداد، بغداد، العراق

**الخلاصة**

تتضمن هذه الدراسة التحقق من سلوك العتبات الخرسانية المدعمة بقضبان طولية وعرضية مصنوعة من البوليمر المقوى بالألياف الزجاجية (GFRP) أو الفولاذ مختبرياً وعددياً. جميع العتبات الخرسانية لها نفس الأبعاد بطول 2700 ملم وعرض 180 ملم وعمق 260 ملم، وقد تم تصنيف العتبات إلى مجموعتين بمتغيرات مختلفة ومقارنة مع عتبة خرسانية مرجعية مقواة بقضبان طولية وعرضية من الفولاذ. تتكون المجموعة الأولى من عتبتين خرسانتين مع قضبان GFRP طولية وبدون اترية، والمتغير في هذه المجموعة هو نسبة التسليح الرئيسية. تتكون المجموعة الثانية من عتبتين خرسانتين مع قضبان GFRP في الاتجاه الطولي واترية مصنوعة من GFRP أو فولاذ في الاتجاه العرضي، والمتغير في هذه المجموعة هو نوع الاترية. أشارت النتائج إلى أن العتبة التي تحتوي على قضبان GFRP حسنت من قوة الانحناء بنسب مختلفة، ولكن كانت مقاومة القص محدودة عند استخدام اترية GFRP لأن زيادة الهطول يؤدي إلى زيادة عدد الشقوق وعرضها مما يقلل من قوة القص. أظهرت جميع العتبات المختبرة سلوكًا مرنًا خطيًا حتى الفشل، حيث كان GFRP أكثر هشاشة من الفولاذ نظرًا لعدم وجود نقطة تحمل أو سلوك بلاستيكي في GFRP. أظهرت المحاكاة العددية للعتبات الخرسانية الخمسة باستخدام برنامج ABAQUS توافق جيد مع البيانات التجريبية التي تم الحصول عليها في المختبر.

**الكلمات المفتاحية:** الالياف الزجاجية المقواة بالبلاستيك، انثناء، انحراف، الخرسانة، القص.

## 1. INTRODUCTION

Concrete is frequently used in many engineering applications for its excellent compressive strength, longevity, and affordability. However, it has a poor tensile strength under service loads or environmental factors. It is prone to breaking. A reinforcement approach with steel bars is adopted to improve the structural performance of the concrete beams. However, steel bars are also susceptible to corrosion, which can reduce their strength and bond with concrete over time. Installing steel bars requires power and specialized equipment due to their weight. An alternative reinforcing method for concrete beams is the Fiber-Rainforced Polymer FRP. Glass fiber Reinforced Polymer GFRP is a composite material made of glass fibers inserted in a polymer matrix. It is one kind of fiber-reinforced Polymer FRP. Compared to steel bars, they are lightweight, corrosion-resistant, easy to install, and have a high tensile strength. Moreover, steel bars are heavy and require special equipment and labour for installation. An alternative solution to reinforce concrete beams is to use fiber-reinforced polymer (FRP) bars. One of the type of fiber-reinforced polymer (FRP) is glass fiber-reinforced polymer (GFRP), a composite material consisting of glass fibers embedded in a polymer matrix. They have several advantages over steel bars, such as high tensile strength, corrosion resistance, lightweight, and ease of installation. By offering corrosion resistance, weight reduction, and crack control under environmental and service loads, the GFRP can improve

the durability performance of concrete beams **(Yost et al., 2001; Shin et al., 2009; Lin and Zhang, 2013; Said and Abbas, 2013).**

Therefore, GFRP bars are promising for reinforcing concrete beams in various applications. As well as there are researchers such as **(Krasniqi et al., 2019; Saleh et al., 2019; Mohammed and Said, 2022)** who have explored the bearing capacity and deflection of concrete beams reinforced with GFRP and steel bars in recent years. For instance, **(Kabashi et al., 2018)** performed an experimental study on the flexural behavior and cracks of concrete beams reinforced with GFRP bars and steel bars. They found that GFRP bars had a lower stiffness and bond capacity than steel bars, which led to larger deflections and crack widths. They also suggested a theoretical correlation for predicting crack width based on their experimental results and previous studies. **(Krasniqi et al., 2019)** examined the flexural capacity and behavior of geopolymer concrete beams reinforced with GFRP bars and ordinary Portland concrete beams reinforced with GFRP bars. They noticed that geopolymer concrete had a higher compressive strength, modulus of elasticity, and bond strength than ordinary Portland concrete, which improved the performance of GFRP-reinforced beams in terms of cracking, deflection, ultimate capacity, and failure mode. A numerical study using the nonlinear finite element program ABAQUS was conducted by **(Mohammed and Said, 2022)** on eight beam models with different parameters such as stirrup spacing, compressive strength, reinforcement layer, and bar type. They discovered that the GFRP beam had a higher ultimate load capacity than the steel-reinforced beam. Still, a higher deflection **(Kinjawadekar et al., 2023)** also arrives at the same result and behavior.

**(Moawad and Fawzi, 2021)** studied the performance of concrete beams partially or fully reinforced with glass fiber polymer bars. They tested six concrete beams with different reinforcement ratios, concrete compressive strength, and GFRP bar types under four-point loading. They found that the GFRP-reinforced beams had higher ultimate load capacity, lower deflection, and smaller crack width than the steel-reinforced beams. They also observed that partial reinforcement with GFRP bars was more effective than full reinforcement regarding ductility and crack control. Studies carried out by different researchers **(Yoo et al., 2016; Ju et al., 2017; Liu et al., 2019; Gora, 2022; Abbood et al., 2021; Ifrahim et al., 2023; Attia et al., 2023)** found that GFRP bars suffered in most of the practical experiments from the low modulus of elasticity and high deflection. In addition, many previous studies conducted by many researchers, such as **(Sundarraja and Rajamohan, 2009; Kaszubska and Kotynia, 2021; Dutta et al., 2022; Sawant and Jadhav, 2022; Fouad et al., 2023; Irmawaty et al., 2023)**, Proves that the ability of concrete beams reinforced with GFRP bars is higher in supporting load capacity than that of steel but, GFRP bars exhibit lower shear force resistance **(Kumari et al., 2018; Kumari and Nayak, et al., 2021).**

This study aims to perform an experimental and numerical investigation of the structural behavior of concrete beams reinforced with longitudinal and transverse GFRP bars and compare them with those of concrete beams reinforced with conventional steel bars. The effects of GFRP bar orientation on the load-deflection relationship, failure mode, flexural capacity, and shear strength are analyzed and discussed.

## 2. EXPERIMENTAL PROCEDURE

### 2.1 Specifications of the Beams under Test

The experimental program consisted of testing five beams under four-point loading. The beams were divided into two groups with different variables: the main reinforcement ratio and the stirrup type (steel or GFRP). All beams had the same dimensions of 2700 mm in length, 180 mm in width, and 260 mm in depth, with a clear span of 2500 mm. The first group comprised two beams with longitudinal GFRP bars and no stirrups labeled G2 and G4. The

second group consisted of two beams with longitudinal GFRP bars and transverse GFRP or steel stirrups labeled B.G2 and B.S2. The last beam, a reference for the other groups, was reinforced with longitudinal and transverse steel bars labeled as Cont. **Fig. 1** and **Table 1.** show the details of all the tested beam specimens.

**Table 1**. Details of all beams.

| Groups | Sample | Spacing | Type of stirrups | Bar top | Bar bottom |
|---|---|---|---|---|---|
| Group 1 | G2 | N/A | N/A | 2 Ø 8 mm | 3 Ø 10 mm |
| | G4 | N/A | N/A | 2 Ø 8 mm | 4 Ø 12 mm |
| Group 2 | B.S2 | 110 mm | Steel - Ø 8 mm | 2 Ø 8 mm | 3 Ø 12 mm |
| | B.G2 | 110 mm | GFRP - Ø 8 mm | 2 Ø 8 mm | 3 Ø 12 mm |
| Control | Cont. | 110 mm | Steel - Ø 8 mm | 2 Ø 8 mm | 3 Ø 12 mm |

*N/A: not applicate

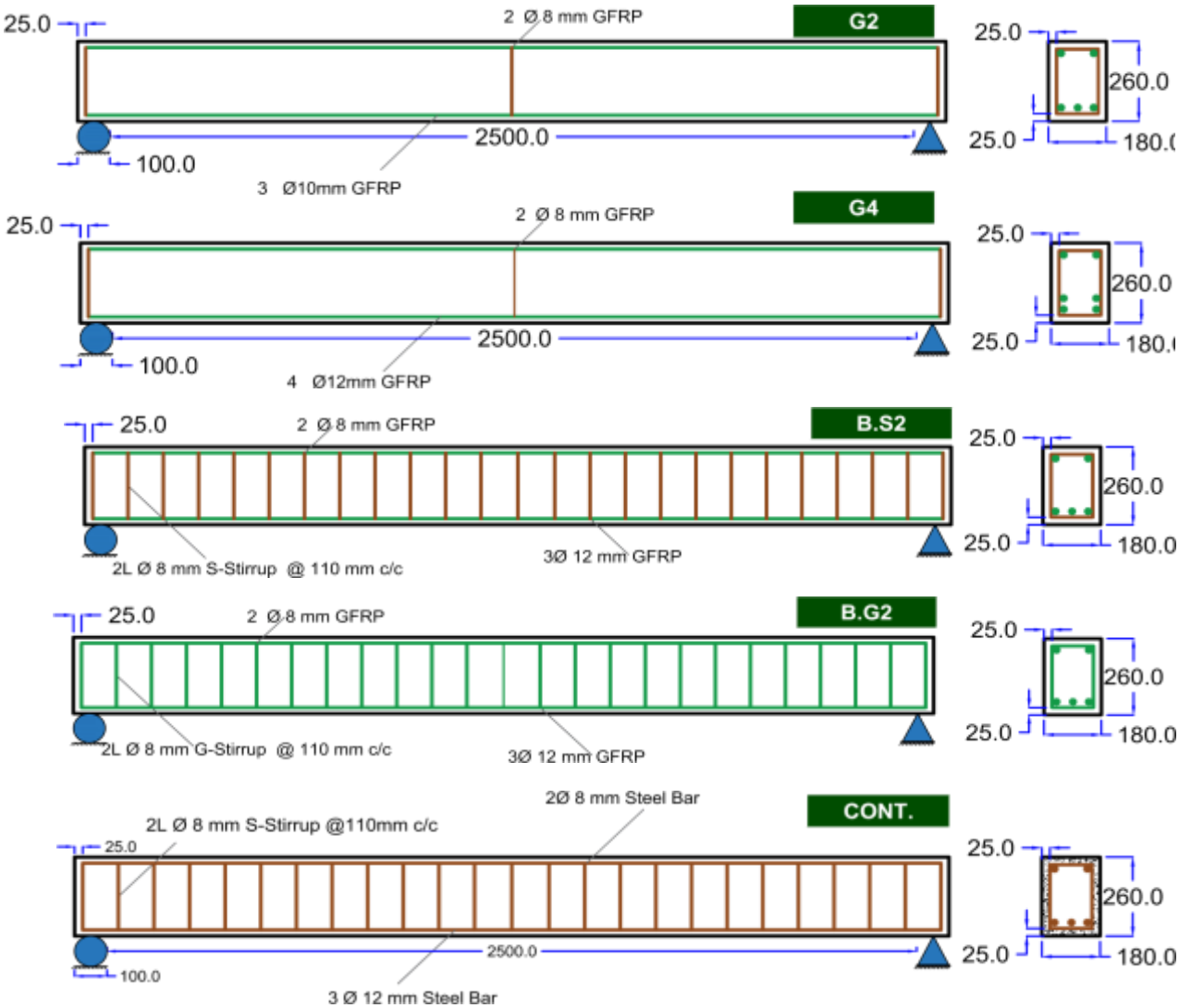


**Figure 1.** Details of all beams.

## 2.2 Material Properties

### 2.2.1 Concrete

The concrete mix was designed according to **(ACI 211.1-22, 2022)** standards to achieve a compressive strength of 40 MPa. The mix components were sand, gravel, cement, water, and some chemical admixtures to enhance the workability without compromising the strength of the hardened concrete. **Table 2** presents the concrete mix proportions for one cubic meter of this material.

**Table 2**. Proportions of the concrete mix components.

| Cement kg/m$^3$ | Gravel kg/m$^3$ | Sand kg/m$^3$ | Water liter/m$^3$ | Silica kg/m$^3$ |
|---|---|---|---|---|
| 475 | 1030 | 640 | 170 | 20 |

### 2.2.2 GFRP and Steel Properties

The longitudinal reinforcement consisted of GFRP bars of 8 , 10, and 12 mm diameters. The stirrups are closed loops of GFRP with a diameter of 8 mm. The tensile properties of the GFRP bars are determined by **(ASTM D7205/D7205M, 2021)**, as shown in **Fig. 2**. The GFRP bars exhibited high tensile strength for different diameters. To prevent the GFRP bars from slipping out of the testing machine due to their high strength, they were inserted into steel tubes of fixed lengths and bonded with epoxy adhesive (sikadur-330) from Sika Company, as shown in **Fig. 2**.

**Figure 2**. Details of tensile test.

The steel tubes followed the ASTM requirements for dimensions and quality. The manufacturer's manual reported a modulus of elasticity of 70000 MPa for all GFRP bars. Due to their high tensile strength and low elastic modulus, GFRP bars exhibit brittle behavior and unexpected failure, but the modulus of elasticity in steel is high **(ACI 440.IR-15, 2015)**. The characteristics of GFRP and steel bars are shown in **Table 3,** which includes the results of the tensile tests on GFRP and steel bars. The Laboratories of the Consulting Office at the College of Engineering, University of Baghdad, conducted all the tensile test.

**Table 3**. Tensile strength of GFRP and steel bar.

| Bar | Tensile Strength $f_y$ (MPa) | Yield strength | Rupture Strain ε | Modulus of Elasticity E (MPa) |
|---|---|---|---|---|
| GFRP | 1350 | N/A | 0.0192 | 70000 |
| Steel | 610 | 450 | 0.0026 | 200000 |

*N/A: not applicate

### 2.3 Testing Process

The laboratory setup for the test consists of a frame with supports spaced according to the design specifications. The specimen geometry specifications are 2700 mm long, 2500 mm span between the supports, the width of support is 100 mm, and the shear span-to-beam depth ratio is about 3.77. Welded supports hold up the specimens. Rubber pads and a spirit level are used to level and stabilize these specimens. The specimens are painted with a light white color to enhance the visibility of cracks during the test. Strain gauges are attached to the specimens in bending and shear stress regions, as well as an LVDT to measure the deflection. The specimens are lifted and placed on the frame, and a hydraulic jack and a load cell are mounted on an I-section above them. The measuring devices are connected to a computer and a data logger. A preliminary test is performed to check the accuracy of the strain gauges and the LVDT. The specimens are subjected to an incremental loading of 250 kg per stage until the hydraulic jack fails. The specimens are observed for crack formation and propagation under the applied loads, and the cracks are marked with black lines along with the corresponding load values. The test results are recorded by the data logger in tabular form, containing hundreds of thousands of data points until the ultimate failure of the specimens. **Fig. 3** shows the details of the test setup components, and **Fig. 4** shows the distance between loads and the shear zones.

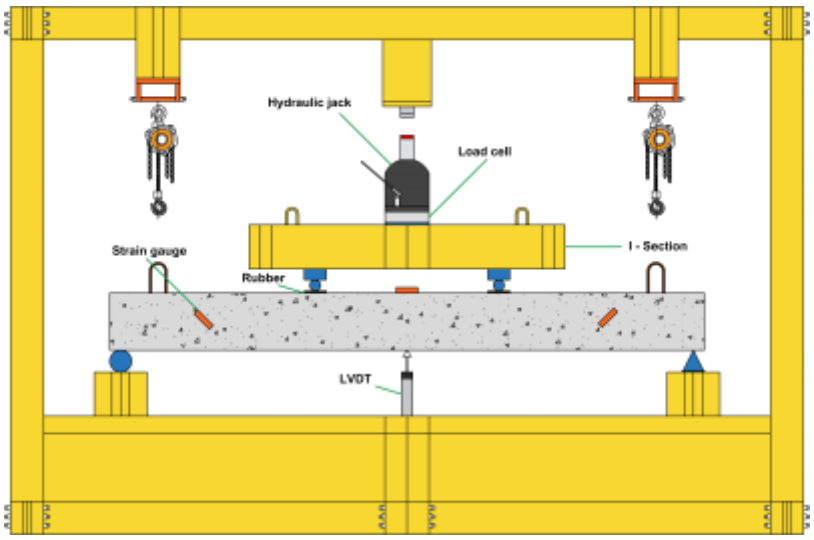


**Figure 3**. Characteristics of parts of the experimental device.

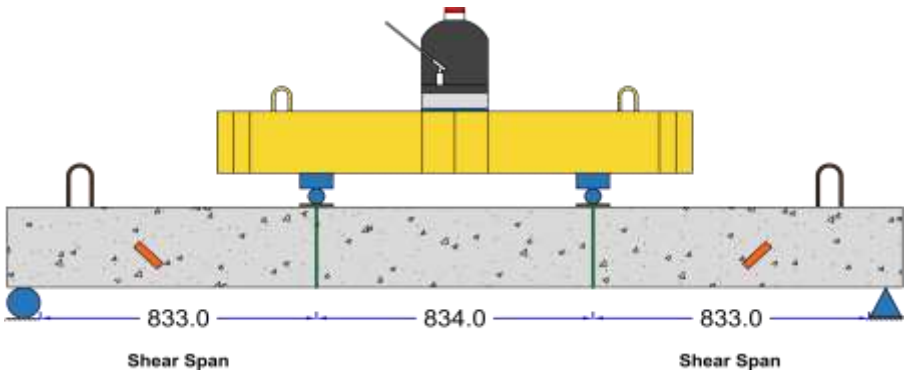


**Figure 4**. Distance between loads and the shear zones.

## 3. FINITE ELEMENT SIMULATION

The beams were modeled using ABAQUS and various theories to simulate four-point bending to investigate the behavior of GFRP and obtain reliable scientific results. The models of the materials were based on their properties and the adopted theories, which were divided into two parts. The first part involved the representation of concrete using the concrete damaged plasticity model, which is more accurate than the smeared cracking model. The second part involved the presentation of steel using the classical theory of metal plasticity, which is based on the von Mises yield criterion and GFRP elastically linearly **(Shin et al., 2009; Said and Abbas, 2013; Genikomsou and Polak, 2015; Metwally, 2017; Pasiou and Kourkoulis, 2018)**. The beam components included GFRP, steel, stirrups, and bearing plates. These components were assigned the material properties defined in the property field, where the elastic and plastic behavior of concrete, GFRP, and steel was specified. The modulus of elasticity and Poisson's ratio were also defined for concrete. The bearing plates were assumed to be made of elastic steel. The beam components were assembled in the next phase of the modeling process, and the static loads applied to the beams were defined. The bond between GFRP and concrete was assumed to be ideal, and the interaction between all beam sections was described. The boundary conditions for the roller and hinge supports were also defined. The meshing phase involved some attempts to find the optimal mesh size and shape, with satisfactory results.

The finite element theories rely on parameters that reflect the general properties of concrete in its common state. These parameters were determined by extensive research and investigations on concrete behavior **(Allawi and Ali, 2020; Ali and Allawi, 2021; Gemi et al., 2021; Mohammed and Said, 2022; Golham and Al-Ahmed, 2023; Ibrahim and Allawi, 2023)**. The concrete damage plasticity data used in the models are given in **Table 4**.

**Table 4**. Concrete damage plasticity.

| parameters | ψ | ϵ | fb0/fc0 | $K$ | μ |
|---|---|---|---|---|---|
| values | 45 | 0.1 | 1.17 | 0.668 | 0.0001 |

## 4. RESULTS AND DISCUSSION

The bending load resistance of four concrete beams is tested and found to be satisfactory. The deflection is reduced, compared with the results of the control beam, reinforced with steel bars in the longitudinal and transverse directions. However, the GFRP shear force resistance was limited. The failure modes and the crack numbers varied with the stirrup type. The beam stiffness increased with GFRP stirrups. The longitudinal reinforcement ratio also affected the deflection and the shear force resistance. A higher percentage resulted in lower deflection due to dowel action and higher shear force resistance.

### 4.1 Fracture Mode and Patterns of Cracks

The first group's beams (G2, G4) mainly failed due to shear stress. The G2 beam exhibited the first crack at a load of 7.5 kN, about 6.9% of the ultimate load capacity. The crack was vertical and outside the bending moment region, near the support in the shear region. As the load increased, more cracks appeared between the two load points in the middle of the beam and extended in length. At a load of 40 kN, the cracks propagated in the shear regions and became slightly inclined near the supports. After reaching about 45% of the ultimate load

capacity, the concrete cover of the beam started to split, with horizontal and diagonal cracks in the shear region. These cracks continued to grow until the beam reached the maximum load capacity and failed abruptly in shear at a load of 109 kN. The concrete cover splitting resulted from to loss of bond between the GFRP bars and the concrete, also due to the increased dowel action from the resistance of the GFRP bars to the shear forces in the beam. When the beam is subjected to a gradually increased load, some shear forces are generated inside the beam. Still, some of these forces were resisted by dowel action from the longitudinal reinforcement with GFRP bars. The longitudinal reinforcement was supported by a concrete cover at the bottom of the beam that resisted the forces (dowel action and displacement) and thus created vertical compression and tension on the concrete, which resulted in diagonal tensile stresses on the concrete and, consequently, concrete cover splitting. **Fig. 5** shows the details of the failure pattern of G2.


**Figure 5**. Failure pattern of G2 beam.

The first crack in the beam (G4) occurred at a load of 12.5 kN, about 11.9% of the ultimate load capacity. The crack was vertical and in the middle of the beam between the two load points. As the load increased, more vertical cracks appeared in the bending moment region. Then, cracks started to appear below the load points at a load of 35 kN, and then the cracks grew in length and width in the regions near the shear regions near the supports until the beam failed suddenly in shear at a load of 105 kN.

In this beam, the shear strength decreased by about 3.67% due to the beam's reduced effective depth due to using two layers of GFRP bars instead of one layer in the longitudinal direction in the tensile region. The overall failure pattern was similar to the previous beams in the same group. In beam (G4), the concrete cover splitting was caused by dowel action from the longitudinal GFRP bars that resisted shear forces. The cracks were narrower than in the previous beams in the same group because of the increased longitudinal reinforcement ratio of the GFRP bars and their distribution in two layers instead of one layer, which increased the stiffness of the beam and reduced the number and width of cracks. **Fig. 6** shows details of the failure pattern of G4. In the second group, the main reinforcement in the longitudinal direction for both beams (B.S2 and B.G2) was GFRP bars with the same ratio (1.5ρ), which made them over-reinforced. The transverse direction had stirrups of either steel or GFRP. The type of stirrups was the main variable for this group.

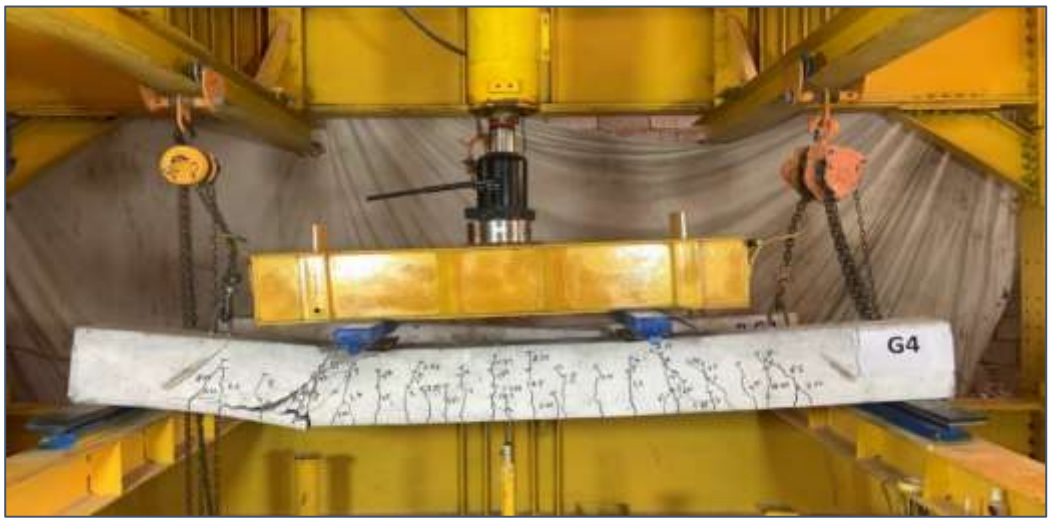


**Figure 6**. The Failure pattern of G4 beam.

In Beam (B.S2), the first cracks appeared vertically at an angle of 90 degrees in the tension area at a load of 15 kN, which is about 10.20% of the ultimate load capacity. The cracks continued to increase below the bending moment area and began to spread towards the shear and compression areas at an escalating pace with the gradual increase in loads until the model failed suddenly at 147 kN by crushing the concrete, known as compression failure. **Fig. 7** shows details of the failure pattern of B.S2.

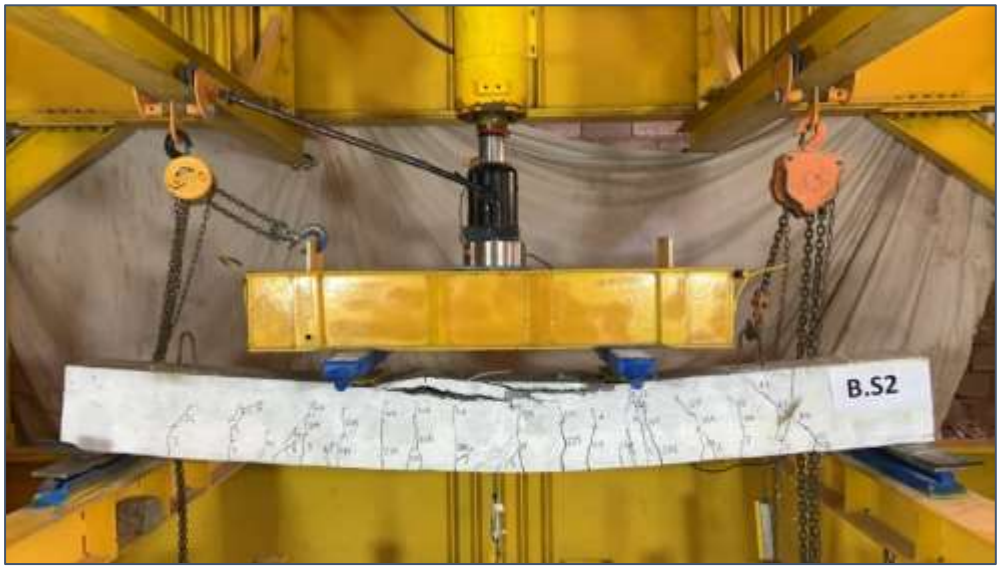


**Figure 7**. The Failure pattern of B.S2 beam.

The beam (B.G2) experienced a sudden shear collapse at 145 kN load. The initial crack appeared vertically in the tension zone at 17.5 kN of load, 12% of the ultimate load capacity. The cracking process progressed steadily in the flexural zone between the two loading points. The cracks extended to the shear zone, where they became diagonal until the failure stage, marked by a sudden shear at a distance (d) from the support face and at a 45-degree angle with concrete cover splitting. Unlike the (B.S2) beam reinforced with steel stirrups, the

failure mode was a shear failure. This could be attributed to several factors, such as the low compressive strength of the GFRP and the lap splice failure in the bent region of stirrups. Although the longitudinal reinforcement is the same in the two concrete beams and the reinforcement in the transverse direction is also similar in terms of the spacing between the stirrups with different types of stirrups, the beam reinforced with steel stirrups showed higher resistance to shear forces. It kept the beam B.S2 resistant to shear until it failed due to compression represented by concrete crushing. However, the matter was different in the beam reinforced with GFRP stirrups, where the GFRP bars showed a noticeable weakness in resisting shear and compression forces due to their low modulus of elasticity. Thus, beam B.G2 failed due to shear at a load of 145 KN which is less than the load that failed at the beam B.S2 by 1.36%, and that is because GFRP stirrups cannot withstand greater shear forces that reach the beam to a stage of failure similar to the failure of beam B.S2. **Fig. 8** illustrates the failure mode of B.G2.

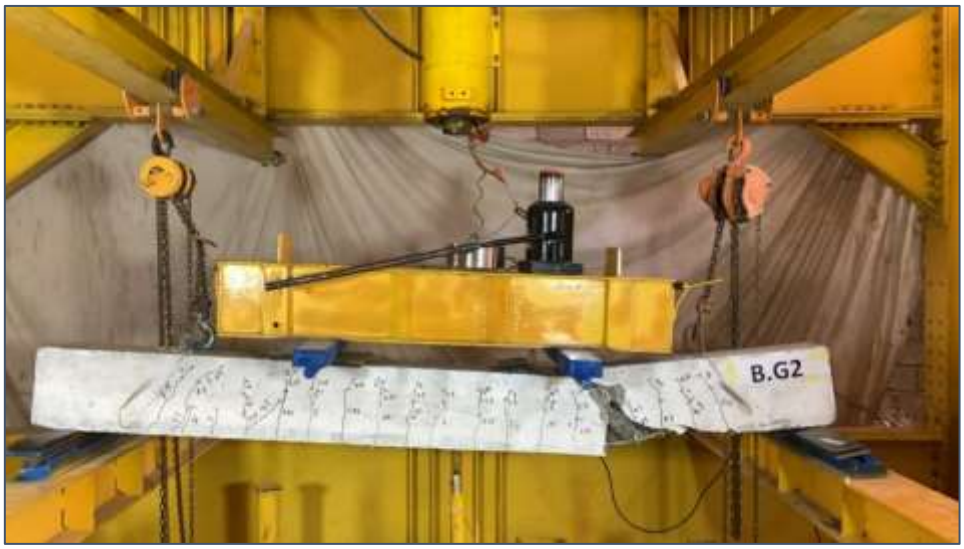


**Figure 8**. The failure pattern of B.G2 beam.

Beam (Cont.) was reinforced with steel bars in longitudinal and transverse directions and was a reference. Vertical cracks at 90-degree angles emerged in the tensile zone between the two loading points at the midspan of the beam when the load reached 10 kN. This load corresponded to 10.86% of the ultimate load capacity of the beam. The cracks propagated symmetrically to the right and left within the bending moment zone. As the load increased to 60-65 kN, the cracks became longer and wider, and some of them extended obliquely in the bending-shear overlapping area. More vertical cracks appeared in the tensile zone at the midspan and below the load point zone until the beam failed at 92 kN due to the rupture of the longitudinal steel bars under bending loads. This was a tensile failure, followed by concrete crushing at the midspan of the beam. When comparing the failure behavior of the (Cont.) beam, it can be observed that the GFRP bars have higher strength against bending loads than the steel bars. On all levels, the beams reinforced with GFRP bars showed more resistance against bending loads than the (Cont.) beam reinforced with steel bars in both longitudinal and transverse directions due to the high tensile strength that the GFRP possesses. **Fig. 9** shows the failure mode of the (Cont.) beam.


**Figure 9**. The Failure pattern of Cont. beam.

### 4.2 Load–Deflection

The four-point bending test of the concrete beams involved measuring the load and the midspan displacements at each loading stage. The resulting load-displacement curves revealed a distinct behavior for the beams reinforced with GFRP bars compared to those with all-steel bars. The GFRP-reinforced beams exhibited larger deflections than the steel-reinforced beams, regardless of the orientation of the GFRP bars. This can be attributed to the lower elastic modulus of the GFRP bars relative to the steel bars. The service load deflections were also higher for the GFRP-reinforced beams than for the steel-reinforced beams. Therefore, GFRP-reinforced concrete beams should be designed with serviceability criteria (deflection and cracking) in mind due to the low elastic modulus of GFRP. The type of stirrups, whether GFRP or steel, had a significant and noticeable impact on the load-displacement curves and the stiffness of the beam in general.

The first group consists of two concrete beams reinforced with only GFRP bars in the longitudinal direction, with different ratios and without stirrups, as mentioned. The service load ratio was adopted around 60% of the maximum load for the G2 beam. The results of load-deflection curves are shown in **Fig. 10**.

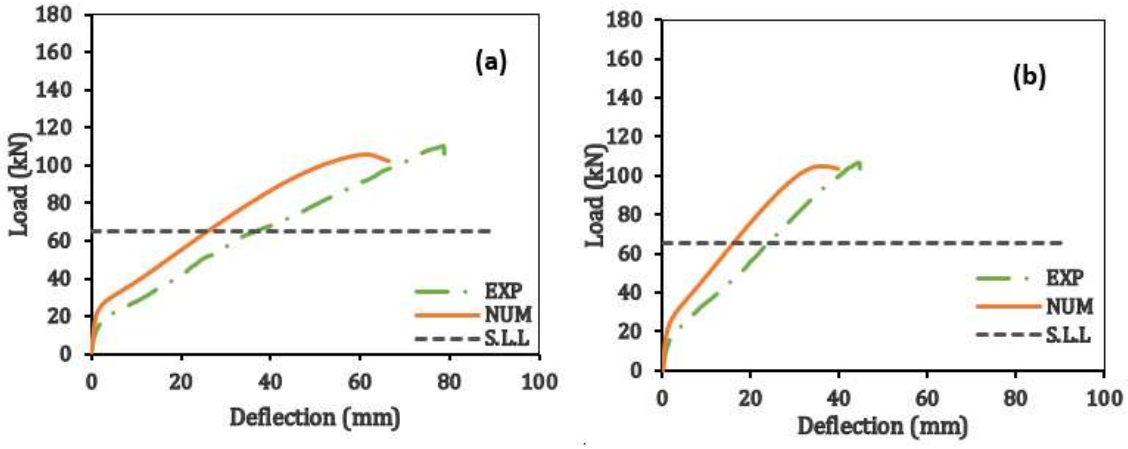


**Figure 10**. Load-deflection details of the beams, (a) for beam G2, and (b) for beam G4.

Increasing the longitudinal reinforcement ratio contributed to reducing (deflection) clearly in the G4 model compared to (deflection) in the G2 model at the service load. It is noted from the curves below that (deflection) in the G4 model decreased by 37% compared to (deflection) in the G2 model due to increasing the longitudinal reinforcement ratio and using two reinforcement layers in the G4 model instead of one layer, which reduced the effective depth slightly. It is also noted from the load – deflection curves the existence of a good match between the experimental and numerical results.

The second group consists of two concrete beams reinforced with GFRP bars in the longitudinal direction and steel and GFRP bars in the transverse direction. As mentioned, the main variable in this group is the type of stirrups used in the transverse reinforcement, whether steel or GFRP. The service load for this group was adopted at a similar ratio to the previous group, which is 60% of the maximum load for beam B.S2. As shown in **Fig. 11**, the results of load-deflection curves showed that the stiffness in the beam reinforced with GFRP stirrups was slightly higher than that in the beam reinforced with steel stirrups at the service load, due to the high tensile resistance that GFRP possesses.

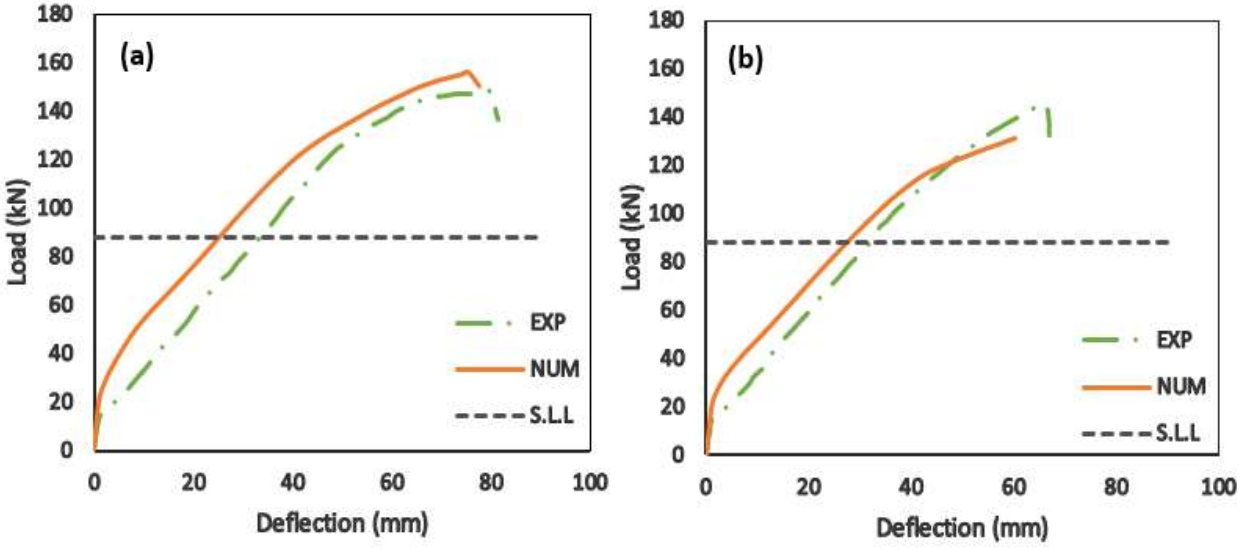


**Figure 11**. Load-deflection details of the beams, (a) for beam B.S2, (b) for beam B.G2.

Despite the weakness of GFRP in the direction of shear and compression forces, the difference in deflection values between the two models was slight, where the deflection in beam B.G2 decreased by about 3% from that in beam B.S2. The results of numerical analysis using the ABAQUS program reported good agreement with the practical aspect.

The failure behavior in the beams was brittle and linear elastic until failure due to the use of GFRP bars in the main reinforcement in both concrete beams. The beam (Cont.) was reinforced with longitudinal and transverse steel bars. The load-deflection curve had two phases: a linear-elastic phase until the steel reinforcement yielded and a nonlinear phase until failure. The service load level (S.L.L) was 60% of the ultimate load on the beam. The deflection at the service load was 7 mm. **Figure 12** shows the load-deflection details of the beam (Cont.).

### 4.3 Load – Strain

Load-strain behavior is an important aspect of the mechanical properties of reinforced concrete structures. Different types of reinforcement, such as steel bars and glass fiber-

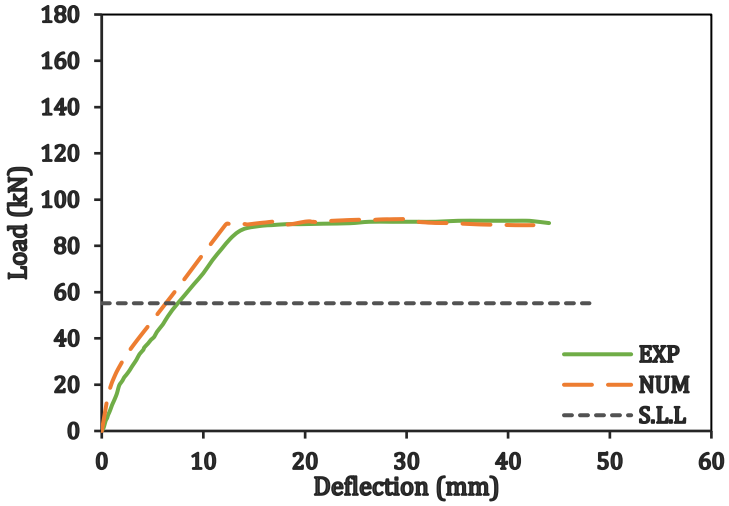


**Figure 12**. Load-deflection details of the beam Cont.

reinforced polymer (GFRP) bars, have different load-strain characteristics under tensile and compressive loading. Steel bars have high elastic modulus and yield strength but are susceptible to corrosion and fatigue. GFRP bars have high tensile strength and corrosion resistance but low elastic modulus and bond strength with concrete. The load-strain curves of steel bars and GFRP bars under repeated tensile loading show different energy-dissipation capacities and residual strains. **Fig. 13** shows the load-strain details of the beams (G2 and G4). G2 and G4 have a linear relationship between load and strain, meaning they obey Hooke's law. However, G4 has a higher stiffness than G2, meaning it can resist more load for the same amount of deformation.

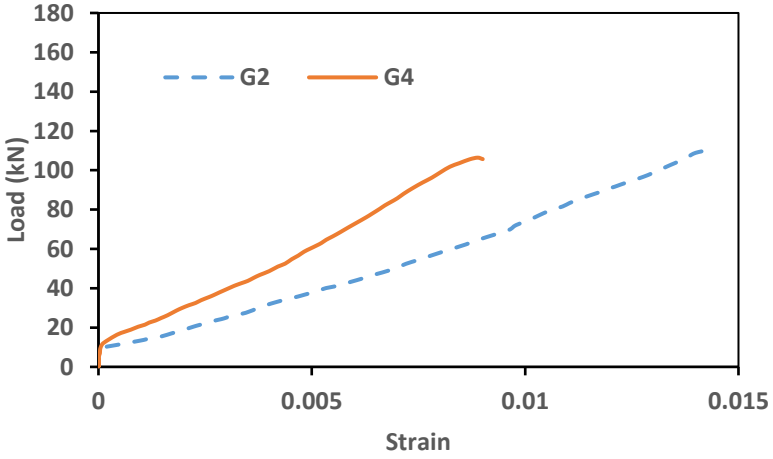


**Figure 13**. Load-strain details of the beams (G2 and G4).

This is evident from the slope of the load-strain curve, which is steeper for G4 than for G2. G4 also has a higher ultimate strength than G2, meaning it can withstand more load before breaking. To quantify the difference between G2 and G4. The percentage difference between

load for G2 and G4 is reported as 3.77%, which is relatively small. However, the percentage difference between strain for G2 and G4 is 35.71%, which is significant. This means that G4 has a slightly lower load but a much lower strain than G2 at the same point of interest. So G4 exhibits superior mechanical performance than G2 in stiffness and strength. **Figure 14** shows the load-strain details of the beams (B.S2 and B.G2) for evaluation the mechanical properties and comparing their load-strain curves. The curves indicated that B.S2 and B.G2 follow Hooke's law, as they have a linear relationship between load and strain. However, B.S2 is stiffer than B.G2, as it can bear more load for the same amount of deformation. B.S2 also has greater ultimate strength than B.G2, as it can endure more load before failing. At a strain of interest, the load for B.S2 is 1.37% higher than that for B.G2, which means that B.S2 has a slightly higher load than B.G2. The strain for B.S2 is 18.75% lower than that for B.G2, which means that B.S2 has a lower strain than B.G2 at the same load of interest.

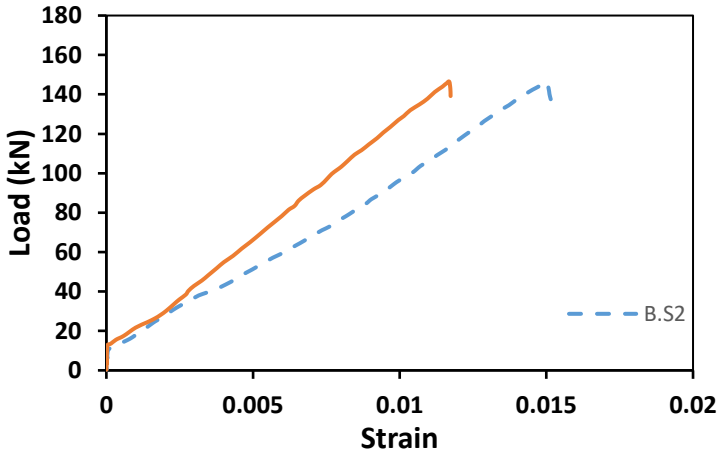


**Figure 14**: load-strain details of the beams (B.S2 and B.G2).

In the Control (Cont.) beam, the curve shows that the load increases linearly with the strain until it reaches a peak value of 92 kN at a strain of 0.0026. This indicates that the steel has a high elastic modulus and can withstand large loads without permanent deformation. However, beyond this point, the curve drops sharply, implying that the steel has reached its ultimate strength and failed due to the rupturing of the steel bar in the tension zone. **Fig. 15** shows the load-strain details of the (Cont.) beam.

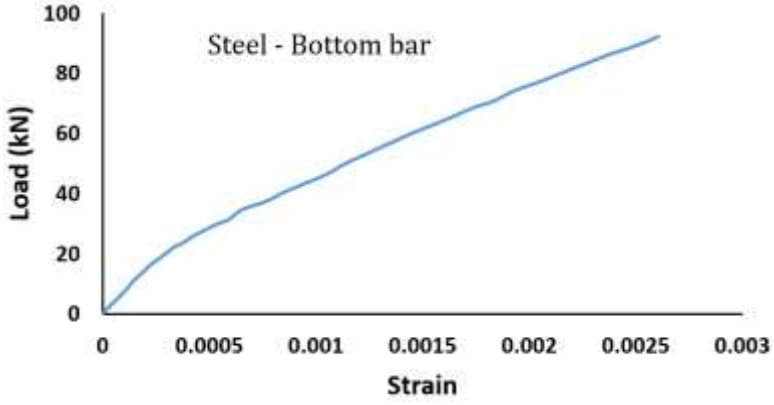


**Figure 15**. load-strain details of the (Cont.) beam.

### 4.4 Numerical Results

The numerical values showed high consistency and accuracy with the experimental data regarding beam load-bearing capacity and ultimate deflection. The numerical validation confirmed that the load-displacement curves had a similar trend to the experimental results. Moreover, the failure mode was also consistent between the experimental and numerical aspects. The results indicated that the FEM was more rigid than the experimental test data. The ultimate loads obtained from the experimental test were lower than the final loads obtained from the FEA, which were considerably higher. These differences were within an acceptable range; thus, the FEM could be used for further studies by changing the parameters of interest. The agreement between the experimental and numerical results in load displacement was satisfactory, as shown in the previous curves. The results of the various analyses in the ABAQUS program were based on several theories and attempts to achieve this accuracy and agreement between the results for the experimental and numerical sides. Since the GFRP had lower compressive strength than the tensile strength, each element in the concrete beams was modeled according to its properties and in a way that was closer to the experimental side. It should be noted that the GFRP stirrups were modeled as solid elements to account for the changes in three directions, not only in compression and tension, and to make the results as realistic as possible. **Fig.16** illustrates the crack pattern of all tested beams using ABAQUS software.

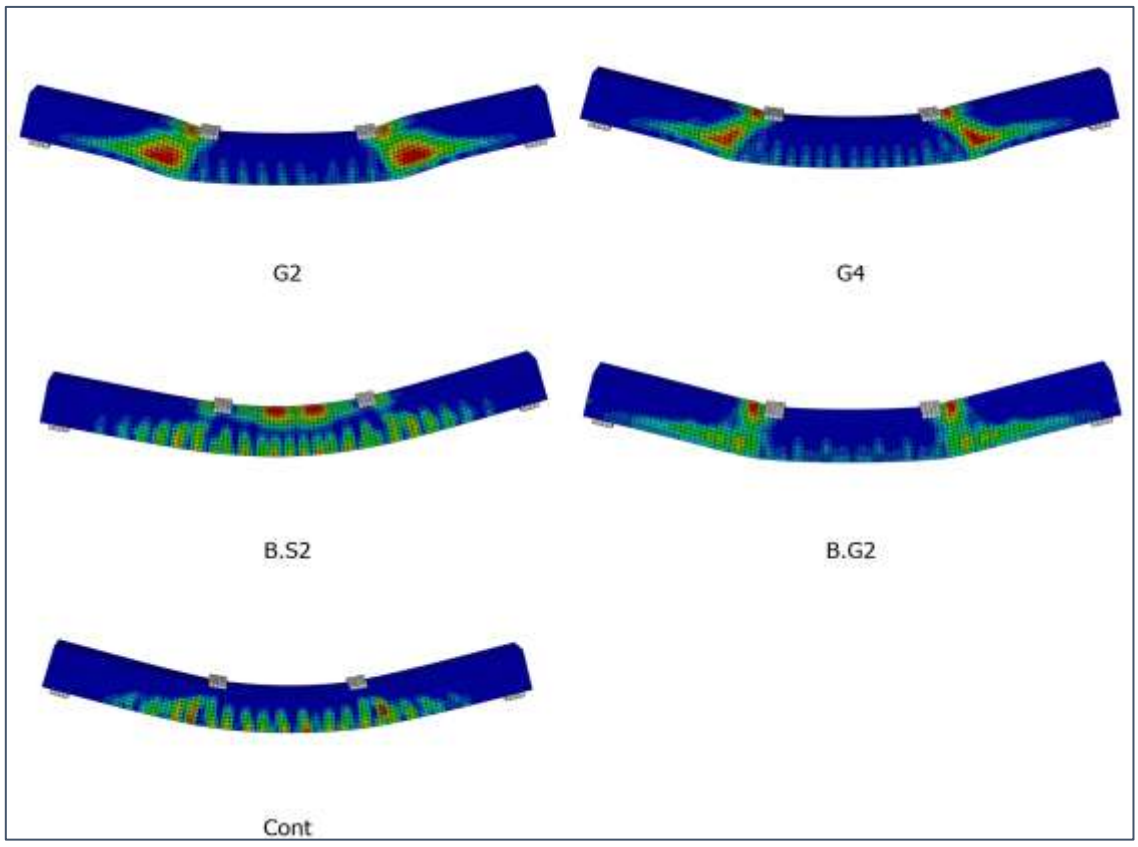


**Figure 16**. Illustrates the crack pattern of all tested beams using ABAQUS software.

## 5. CONCLUSIONS

The results showed generally good behavior of GFRP bars in bearing flexural loads and increasing beam stiffness equally. Despite the weakness of GFRP in bearing shear and compression forces, slipping also increased the effect of shear forces on GFRP bars. The behavior of GFRP was linear elastic until failure due to the low modulus of elasticity that also gave it the characteristic of brittleness, unlike steel which showed high ductility in dealing with the loads applied to it due to the high modulus of elasticity except GFRP distinguished from it by high tensile strength which gave the concrete beam higher bearing capacity for flexural loads.

- The results showed that the beams reinforced with GFRP bars in the longitudinal direction exhibited linear elastic and brittle behavior until failure, whereas the beams reinforced with steel bars in the longitudinal direction displayed ductile behavior with a noticeable softening in the load-deflection curve. This was attributed to the low modulus of elasticity of GFRP bars compared to the high modulus of elasticity of steel bars. The flexural load capacity of the beam reinforced with GFRP bars was 58.70% higher than that of the beam reinforced with steel bars, due to the high tensile strength of GFRP bars compared to steel bars.
- The shear strength of GFRP was found to be lower than that of steel, as indicated by the failure mode of the beam with GFRP stirrups. The beam with steel stirrups had a 3.67% higher resistance to shear forces. The beam reinforced with stirrups from GFRP had wider and more cracks than the beam reinforced with steel stirrups.
- The longitudinal reinforcement ratio with GFRP bars was observed to increase the beam stiffness, especially the flexural stiffness. The use of two layers of GFRP as reinforcement for the concrete beam did not affect the shear resistance area due to dowel action, unlike the single layer that enhanced the shear resistance area. However, the two layers improved the beam stiffness and reduced the deflection by 37.11% at the service load.
- All groups showed a linear relationship between load and strain, meaning they obeyed Hooke's law. The percentage difference between load and strain for G2 and G4 at a point of interest was 3.77% and 35.71%, respectively, indicating that G4 had a slightly lower load but a much lower strain than G2. The percentage difference between load and strain for B.S2 and B.G2 at a strain of interest was 1.37% and 18.75%, respectively, indicating that B.S2 had a slightly higher load but a lower strain than B.G2. Cont. had a high elastic modulus and could withstand large loads without permanent deformation until it reached a peak value of 92 kN at a strain of 0.015, failing due to the rupture of the steel bar in the tension zone.
- The numerical values from FEM agreed well with the experimental data regarding load-bearing capacity and deflection of concrete beams reinforced with GFRP. The load-displacement curves and the failure modes were similar between the experimental and numerical aspects. The FEM was slightly more rigid and predicted higher ultimate loads than the experimental test, but the differences were acceptable.

**NOMENCLATURE**

| Symbol | Description | Symbol | Description |
|---|---|---|---|
| GFRP | glass Fiber Reinforced Polymer | $\psi$ | dilation Angle |
| fb0/fc0 | ratio of biaxial strength to uniaxial strength for concrete | $\epsilon$ | eccentricity |
| $K$ | Shape parameter | $\mu$ | viscosity parameter |

## Acknowledgements

This work was supported by the College of Engineering, University of Baghdad. The authors gratefully acknowledge the PLS lab staff in the Department of Civil Engineering within the College of Engineering. Without their help and contribution, this work would not have been accomplished.

## Credit Authorship Contribution Statement

Shaysh Aziz Mohammed is responsible for collecting data, executing the experimental and numerical simulations, analyzing and interpreting the writing, and reviewing and editing the manuscript. AbdulMuttailb Issa Said supervised, reviewed, and edited the manuscript.

## Declaration of Competing Interest

The authors declare that they have no known competing financial interests or personal relationships that could have appeared to influence the work reported in this paper.

## REFERENCES

Abbood, I.S., Odaa, S.,Hasan, K.F., Jasim, M.A., 2021. Properties evaluation of fiber reinforced polymers and their constituent materials used in structures–A review. *Materials Today: Proceedings*, 43, pp. 1003–1008. Doi:10.1016/j.matpr.2020.07.636.

ACI 440.1R-15, 2015. *Guide for the design and construction of structural concrete reinforced with FRP bars.* Farmington Hills: American Concrete Institute, ACI Committee 440.

ACI PRC-211.1-22, 2022. *Selecting proportions for normal-density and high density-concrete – guide.* American Concrete Institute.

Ali, S.I., and Allawi, A.A., 2021. Effect of web stiffeners on the flexural behavior of composite GFRP-concrete beam under impact load. *Journal of Engineering*, 27(3), pp. 73-92. Doi:10.31026/j.eng.2021.03.06

Allawi, A.A., and Ali, S.I., 2020. Flexural behavior of composite GFRP pultruded I-section beams under static and impact loading. *Civil Engineering Journal*, *6*(11), pp. 2143-2158. Doi:10.28991/cej-2020-03091608

ASTM D7205/D7205M, 2021. *Standard test method for tensile properties of fiber reinforced polymer matrix composite bars*. ASTM International, Volume 15.03, pages 13 Doi:10.1520/D7205_D7205M-21

Attia, M.M., El-Latief, A.A., and Eita, M.A., 2023. Performance of RC beams with novelty GFRP under the bending load: An experimental and FE study. *Case Studies in Construction Materials*, 18, P. e02000. Doi:10.1016/j.cscm.2023.e02000.

Dutta, B., Kumari, A., and Nayak, A.N., 2022. Shear behaviour of RC deep beams retrofitted with externally bonded GFRP fabrics: Experimental and numerical study. *Structures*, 46, pp. 1–16. Doi:10.1016/j.istruc.2022.10.042.

Fouad, R., Aboubeah, A.S., Hussein, A., Zaher, A., Said, H., 2023. Flexural behavior of RC continuous beams having hybrid reinforcement of steel and GFRP bars. *Journal of Reinforced Plastics and Composites*, P. 073168442311516. Doi:0.1177/07316844231151607.

Gemi, L., Madenci, E., and Özkılıç, Y.O., 2021. Experimental, analytical and numerical investigation of pultruded GFRP composite beams infilled with hybrid FRP reinforced concrete. *Engineering Structures*, 244, P.112790. Doi:10.1016/j.engstruct.2021.112790

Genikomsou, A.S., and Polak, M.A., 2015. Finite element analysis of punching shear of concrete slabs using damaged plasticity model in ABAQUS. *Engineering structures*, *98*, pp. 38-48. Doi:10.1016/j.engstruct.2015.04.016

Golham, M.A., and Al-Ahmed, A.H.A., 2023. Behavior of GFRP reinforced concrete slabs with openings strengthened by CFRP strips. *Results in Engineering*, *18*, p.101033. Doi:10.1016/j.conbuildmat.2013.03.023

Gora, A.M., 2022b. *Behaviour of rectangular RC columns confined with bi-directional GFRP under combined axial and bending loadings*. Ph.D. thesis, Department of Civil Engineering, University of Nottingham. https://eprints.nottingham.ac.uk/67463/.

Ibrahim, T.H., and Allawi, A.A., 2023. The response of reinforced concrete composite beams reinforced with pultruded GFRP to repeated loads. *Journal of Engineering*, *29*(1), pp. 158-174. Doi:10.31026/j.eng.2023.01.10

Ifrahim, M.S., Sangi, A.J., and Ahmad, S.H., 2023. Experimental and numerical investigation of flexural behaviour of concrete beams reinforced with GFRP bars. *Structures*, 56, P. 104951. Doi:10.1016/j.istruc.2023.104951.

Irmawaty, R., Fakhruddin, F., Djamaluddin, R., and Kusnad, K., 2023. Failure mode of GFRP bar RC beams using GFRP sheet as shear reinforcement. *Materials Science Forum*, 1091, pp. 101–109. Doi:10.4028/p-602gws.

Ju, M.K., Lee, S.Y., and Park, C., 2017. Response of Glass Fiber Reinforced Polymer (GFRP)-Steel hybrid reinforcing bar in uniaxial tension. *International Journal of Concrete Structures and Materials*, 11(4), pp. 677–686. Doi:10.1007/s40069-017-0212-9.

Kabashi, N., Krasniqi, C., Sustersic, J., Dautaj, A., Krasniqi, E., and Morina, H., 2018. Flexural behavior and cracks in concrete beams reinforced with GFRP bars. Mirmiran, A., and Nanni, A., eds., *International Congress on Polymers in Concrete (ICPIC 2018). Cham: Springer*, pp. 617-625. Doi:10.1007/978-3-319-78175-4_79

Kaszubska, M., and Kotynia, R., 2021. *Accuracy of existing theoretical models on the assessment of the design shear capacity of slender RC beams with steel and GFRP rods without transverse reinforcement. Springer eBooks*, pp. 907–917. Doi:10.1007/978-3-030-88166-5_79.

Kinjawadekar, T.A., Patil, S., and Nayak, G.A., 2023. Critical review on glass fiber-reinforced polymer bars as reinforcement in flexural members. *Journal of The Institution of Engineers (India): Series A*, 104, pp. 501-516. Doi:10.1007/s40030-023-00729-6

Krasniqi, E., Kabashi, N., Krasniqi, C., Dautaj, A., Sustersic, J., and Morina, H., 2019. Flexural capacity and behaviour of geopolymer concrete beams reinforced with GFRP bars. *International Journal of Concrete Structures and Materials*, 13(1), p. 39. Doi:10.1186/s40069-019-0389-1

Kumari, A., and Nayak, A.N., 2021. Strengthening of shear deficient RC deep beams using GFRP sheets and mechanical anchors. *Canadian Journal of Civil Engineering*, 48(1), pp. 1–15. Doi:10.1139/cjce-2019-0333.

Kumari, A., Patel, S., and Nayak, A.N., 2018. Shear strengthening of RC deep beam using externally bonded GFRP fabrics. *Journal of the Institution of Engineers (India): Series A*, 99(2), pp. 341–350. Doi:10.1007/s40030-018-0272-0.

Lin, X., and Zhang, Y.X., 2013. Bond–slip behaviour of FRP-reinforced concrete beams. *Construction and Building Materials*, *44*, pp. 110-117. Doi:10.1016/j.conbuildmat.2013.03.023

Liu, X., Sun, Y., and Wu, T., 2019. Flexural capacity and deflection of fiber-reinforced lightweight aggregate concrete beams reinforced with GFRP bars. *Sensors*, 19(4), p. 873. Doi:10.3390/s19040873.

Metwally, I.M., 2017. Three-dimensional nonlinear finite element analysis of concrete deep beam reinforced with GFRP bars. *HBRC Journal*, *13*(1), pp. 25-38. Doi:10.1016/j.hbrcj.2015.02.006

Pasiou, E., and Kourkoulis, S., 2018. Mechanical response of marble epistyles under shear: numerical analysis using an experimentally validated model. *Journal of the Mechanical Behavior of Materials*, *27*(3-4), 20180023. Doi:10.1515/jmbm-2018-0023

Moawad, M.S., Fawzi, A., 2021. Performance of concrete beams partially/fully reinforced with glass fiber polymer bars. *Journal of Engineering and Applied Science,* 68, P. 38. Doi:10.1186/s44147-021-00028-6

Mohammed, S.A., and Said, A.I., 2022. Analysis of concrete beams reinforced by GFRP bars with varying parameters. *Journal of the Mechanical Behavior of Materials*, *31*(1), pp. 767-774. Doi:10.1515/jmbm-2022-0068

Shin, S., Seo, D., and Han, B., 2009 Performance of concrete beams reinforced with GFRP bars. *Journal of Asian Architecture and Building Engineering*, 8(1), pp. 197–204. Doi:10.3130/jaabe.8.197.

Said, A.I., and Abbas, O.M., 2013. Serviceability behavior of high strength concrete I-beams reinforced with carbon fiber reinforced polymer bars. *Journal of Engineering, 19*(11), pp. 1515-1530. Doi:10.31026/j.eng.2013.11.01

Saleh, Z.S., M.N., Remennikov, A.M., and Basu, A., 2019. Numerical investigations on the flexural behavior of GFRP-RC beams under monotonic loads. *Structures*, 20, pp. 255–267. Doi:10.1016/j.istruc.2019.04.004.

Sawant, S.G., and Jadhav, H., 2022. Flexural behaviour of GFRP strengthened RC beams under cyclic loading. *Materials Today: Proceedings*, 59, pp. 188–195. Doi:10.1016/j.matpr.2021.10.396.

Sundarraja, M.C., and Rajamohan, S., 2009. Strengthening of RC beams in shear using GFRP inclined strips – An experimental study. *Construction and Building Materials*, 23(2), pp. 856–864. Doi:10.1016/j.conbuildmat.2008.04.008.

Yoo, D.Y., Banthia, N., and Yoon, Y.S., 2016. Predicting service deflection of ultra-high-performance fiber-reinforced concrete beams reinforced with GFRP bars. *Composites Part B-engineering*, 99, pp. 381–397. Doi:10.1016/j.compositesb.2016.06.013.

Yost, J.R., Gross, S.P., and Dinehart, D.W., 2001. Shear strength of normal strength concrete beams reinforced with deformed GFRP bars. *Journal of composites for construction*, *5*(4), pp. 268-275. Doi:10.1061/(ASCE)1090-0268(2001)5:4(268).